

⁴⁸Ca CREX

and

²⁰⁸Pb PREX

Robert Michaels

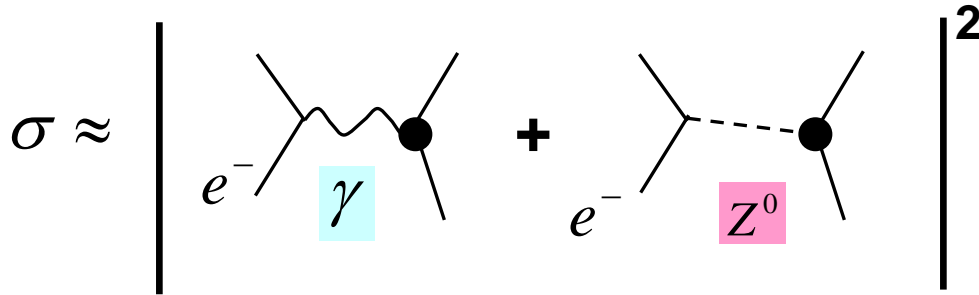
Jefferson Lab

<http://hallaweb.jlab.org/parity/prex>

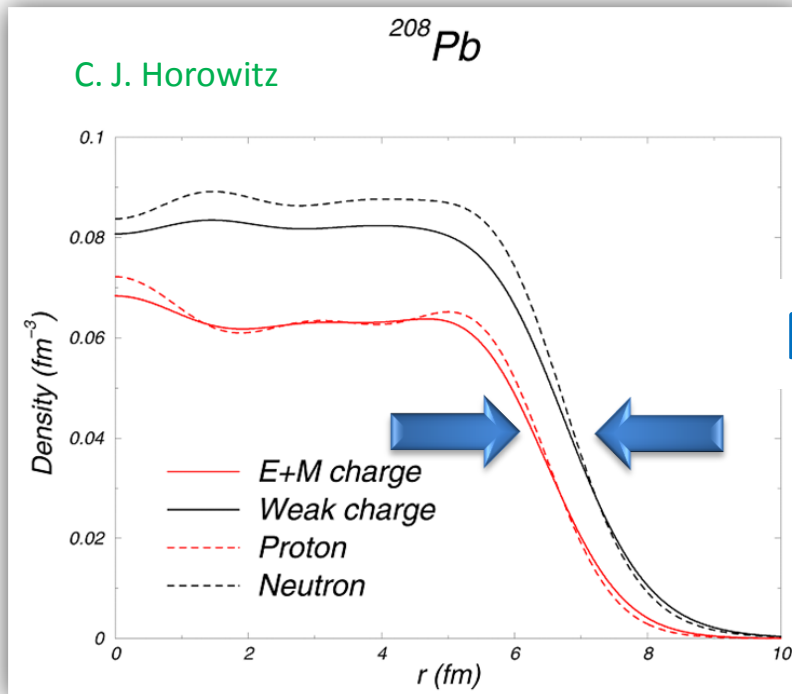
Hall A Collab Mtg, Jan 26, 2023

PRL 129, 042501 (2022)

PRL 126, 172502 (2021)



$$A_{PV} = \frac{\sigma_R - \sigma_L}{\sigma_R + \sigma_L} \sim 10^{-4} \times Q^2 \sim 10^{-6}$$

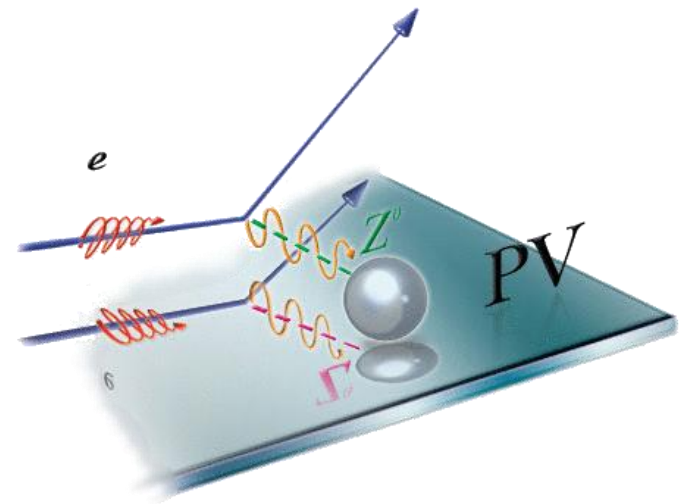


Electroweak Asymmetry in Elastic Electron-Nucleus Scattering

Neutron Skin

$$R_n - R_p = \sqrt{\langle r_n^2 \rangle} - \sqrt{\langle r_p^2 \rangle}$$

The *weak interaction* changes with mirror imaging which allows to isolate it.



Positive spin

Mirror Image



Negative spin

Incident electron

spin



momentum



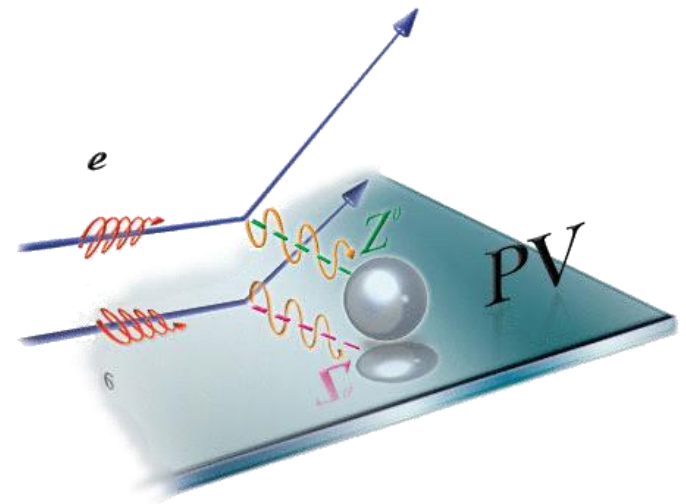
Target



A nucleus in target



The *weak interaction* changes with mirror imaging which allows to isolate it.



Positive spin

Mirror Image



Negative spin

Incident electron

spin



momentum



Target



A nucleus in target



Method: Flip spin of electrons and look for difference in scattering rate.

Using Parity Violation

Electron - Nucleus Potential $\hat{V}(r) = V(r) + \gamma_5 A(r)$

electromagnetic

$$V(r) = \int d^3 r' Z \rho(r') / |\vec{r} - \vec{r}'|$$

forward angle

$$\frac{d\sigma}{d\Omega} = \frac{d\sigma}{d\Omega_{Mott}} |F_P(Q^2)|^2$$

Proton form factor

$$F_P(Q^2) = \frac{1}{4\pi} \int d^3 r j_0(qr) \rho_P(r)$$

Parity Violating Asymmetry

$$A = \frac{\left(\frac{d\sigma}{d\Omega}\right)_R - \left(\frac{d\sigma}{d\Omega}\right)_L}{\left(\frac{d\sigma}{d\Omega}\right)_R + \left(\frac{d\sigma}{d\Omega}\right)_L} = \frac{G_F Q^2}{2\pi\alpha\sqrt{2}} \left[\underbrace{1 - 4\sin^2 \theta_W}_{\approx 0} - \frac{F_N(Q^2)}{F_P(Q^2)} \right]$$

axial

$$A(r) = \frac{G_F}{2\sqrt{2}} [(1 - 4\sin^2 \theta_W) Z \rho_P(r) - N \rho_N(r)]$$

\Rightarrow $A(r)$ is small, best observed by parity violation

\Rightarrow $1 - 4\sin^2 \theta_W \ll 1$ neutron weak charge \gg proton weak charge

Neutron form factor

$$F_N(Q^2) = \frac{1}{4\pi} \int d^3 r j_0(qr) \rho_N(r)$$

Weak Interaction: Sees the Neutrons

	proton	neutron
Electric charge	1	0
Weak charge	0.08	1

Measured Asymmetry



Correct for Coulomb Distortions



Weak Density at one Q^2



Small Corrections for
 G_E^n G_E^S MEC
 surface thickness

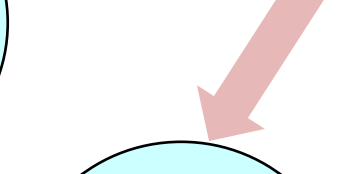
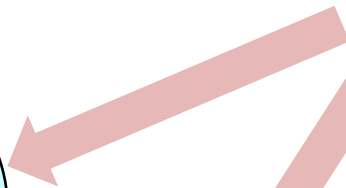


APPLICATIONS

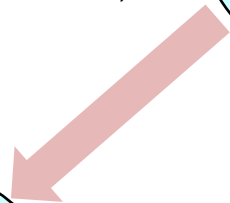
T.W. Donnelly, J. Dubach, and Ingo Sick,
 Nuc. Phys. A 503 (1989) 589.

C.J. Horowitz, S.J. Pollock, P.A.
 Souder, R. Michaels, Phys. Rev. C63,
 025501 (2001)

Nuclear Theory (Symmetry Energy)



Heavy Ions



Neutron Stars

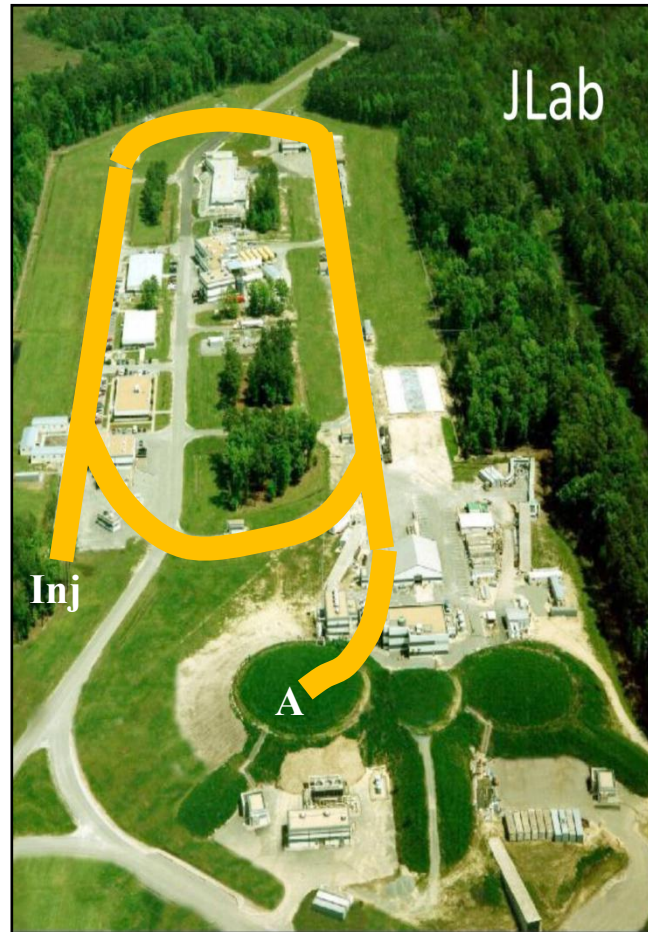
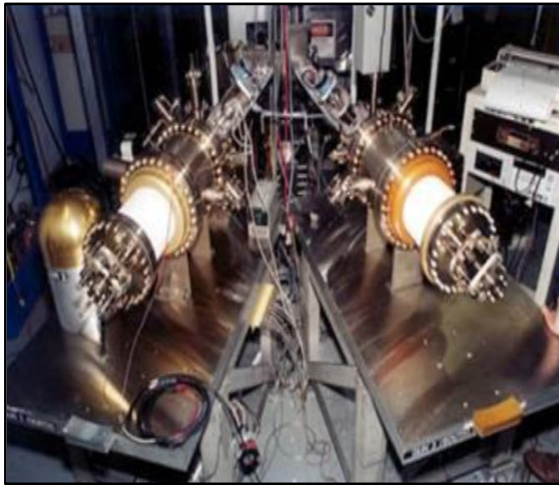


Atomic Parity Violation

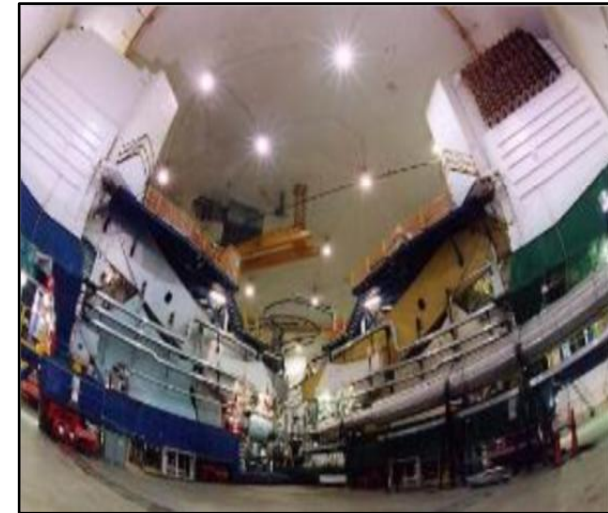
Skin
 $R_N - R_P$

Experimental Overview

**Polarized
Electron
Source**



**Hall A
High Resolution
Spectrometers**



Parity violation experiments at Jefferson Lab use a high-intensity polarized electron beam, with very low beam jitter, and high-resolution spectrometers to isolate elastic scattering.

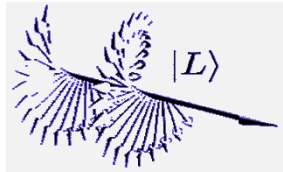
Producing Polarized Electrons

Laser Beam

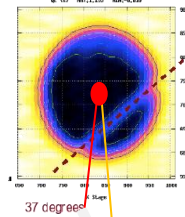
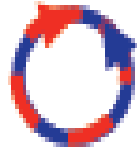
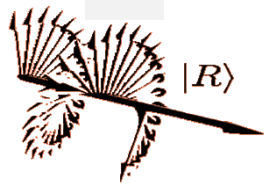
Reversal combinations

Helicity: HV +/-, IHWP out/in

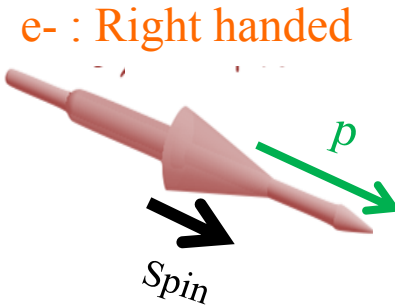
Electron Beam



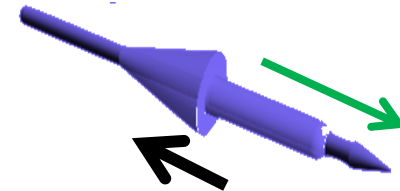
Circularly polarized light



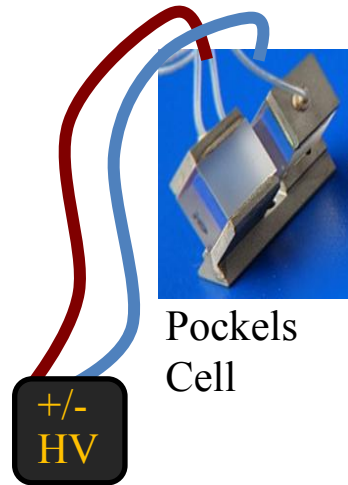
GaAs crystal



e- : Right handed

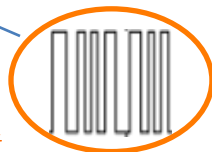


e- : Left handed

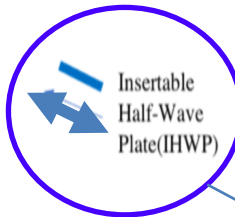


Pockels Cell

Randomized Helicity Signal

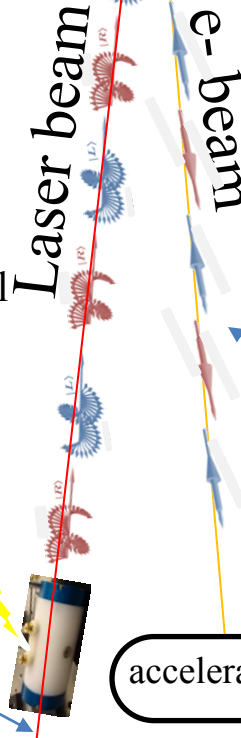


fast

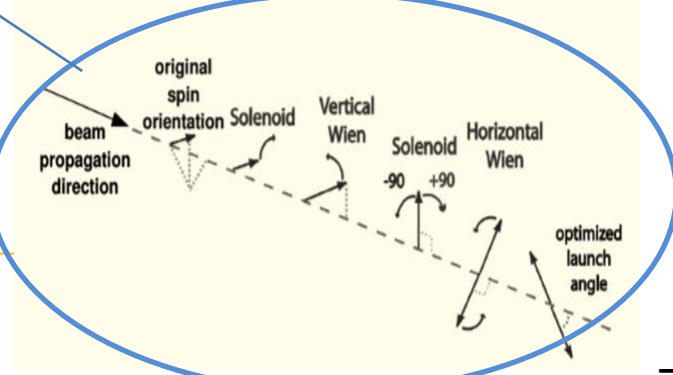


slow

Insertable Half-Wave Plate (IHWP)



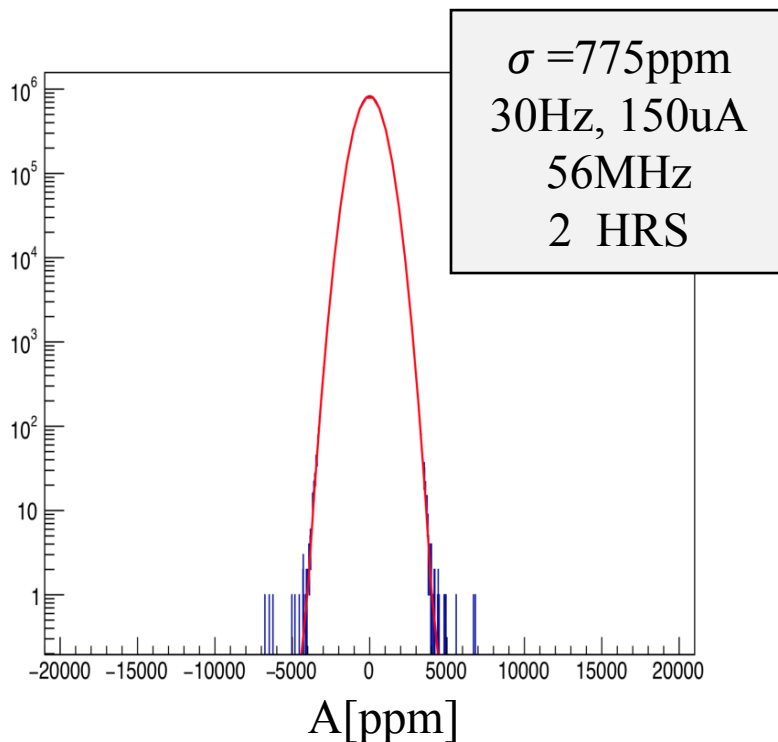
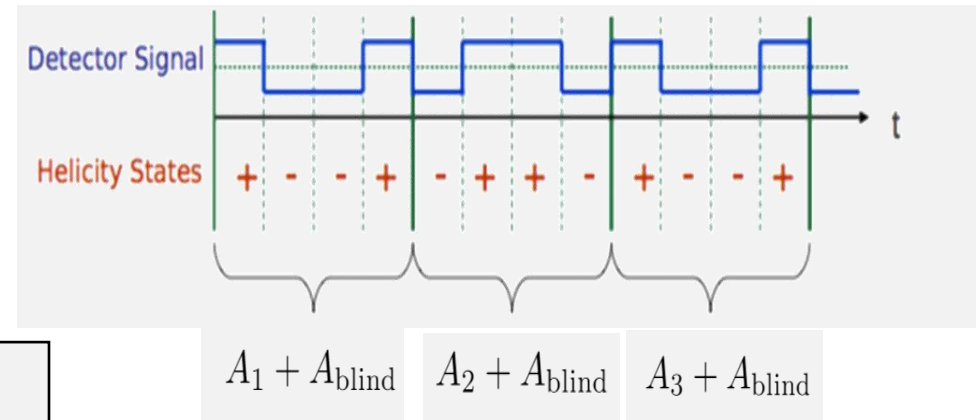
accelerator



Measuring a Small Asymmetry

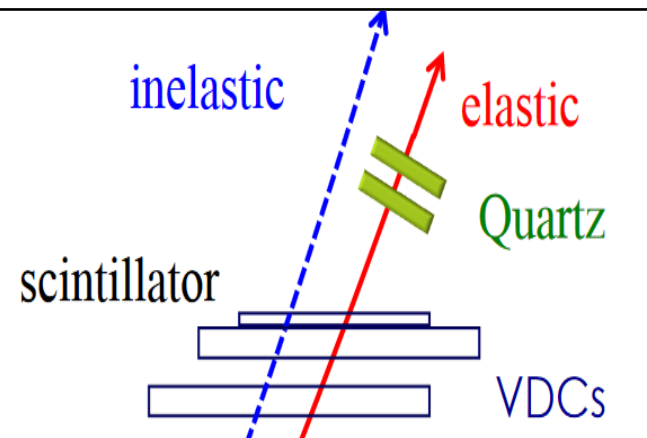
Goal: measure beam-helicity-correlated elastic scattering asymmetry to high precision

$$A_{PV} = \frac{\sigma_R - \sigma_L}{\sigma_R + \sigma_L}$$



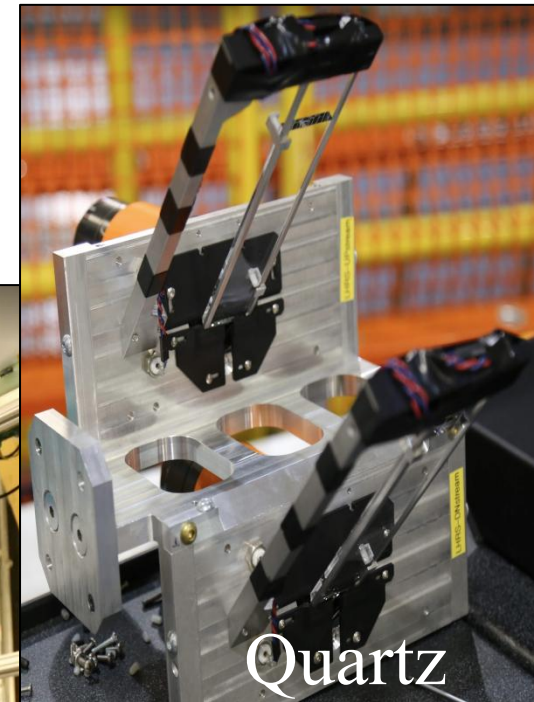
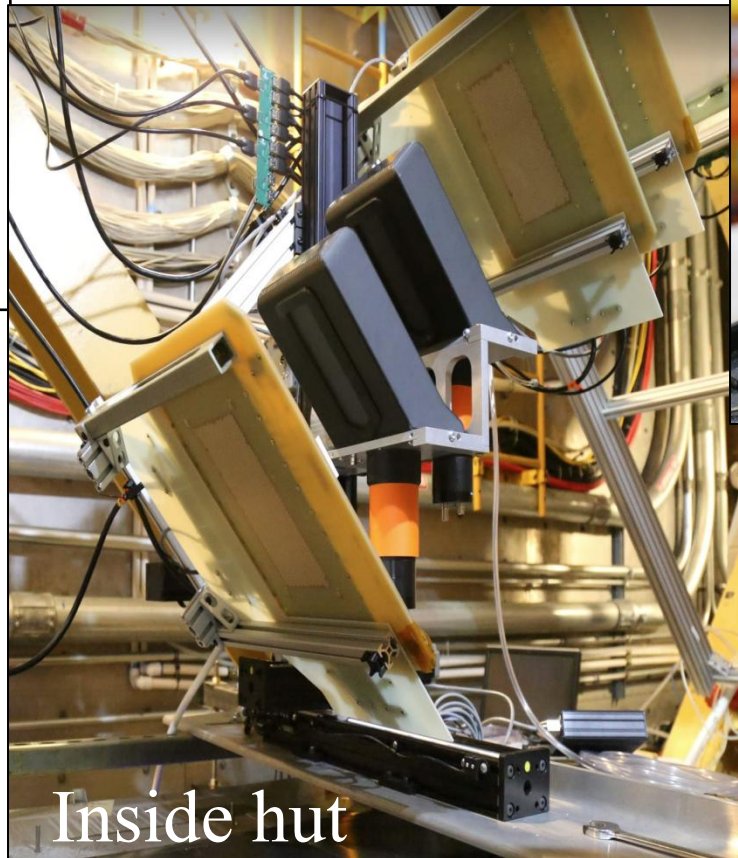
- Integrating, not counting -- total number of detected electrons was $\sim 2.4 \times 10^{21}$, $\sim 383 \text{ C}$
- Online analysis showed we were dominated by counting statistics fairly early in the experiment
- Number of flips ~ 300 million, quartets ~ 80 million
- *Technique built for big rates and small asymmetries (PREX 4GHz, 0.55ppm)*
- *CREX less challenging in terms of rate (CREX 50MHz, 1% of PREX rate, larger asymmetry)*

Detectors at the HRS Focus



“HRS” = high resolution spectrometers

Quartz detectors are placed in the detector hut. They were used for both PREX and CREX.



- Integrating detectors (zero deadtime DAQ)
- Thick and thin quartz bars (different systematics)

Targets : Isotopically pure ^{48}Ca and ^{208}Pb



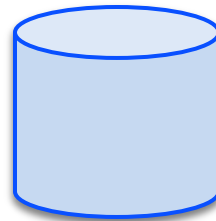
Dave Meekins



Cold target ladder (^{208}Pb and ^{48}Ca)

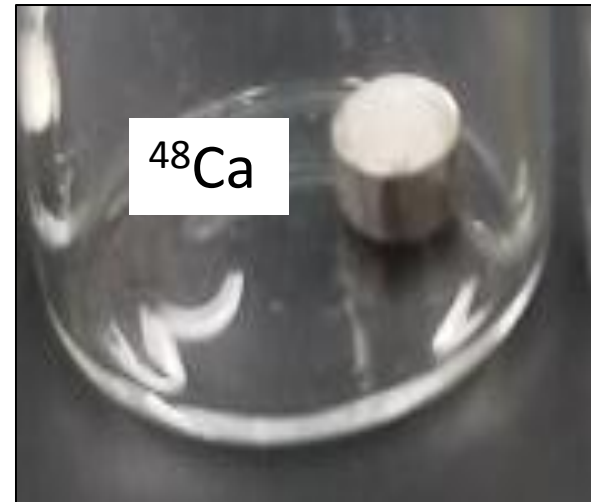
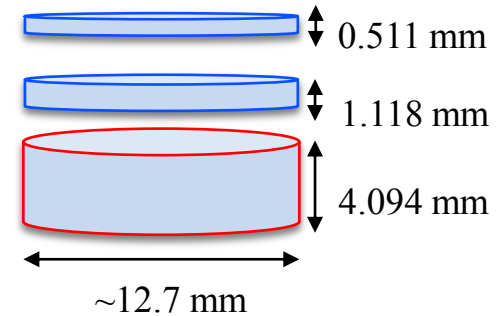
Started with

- Single puck
- 5mm thick
- 96% ^{48}Ca
- 3.84% ^{40}Ca



Ended with

- 1puck+2 foils sandwiched
- ~5.7mm thick total
- ~91.7% ^{48}Ca
- ~7.96% ^{40}Ca



Extracting the Asymmetry

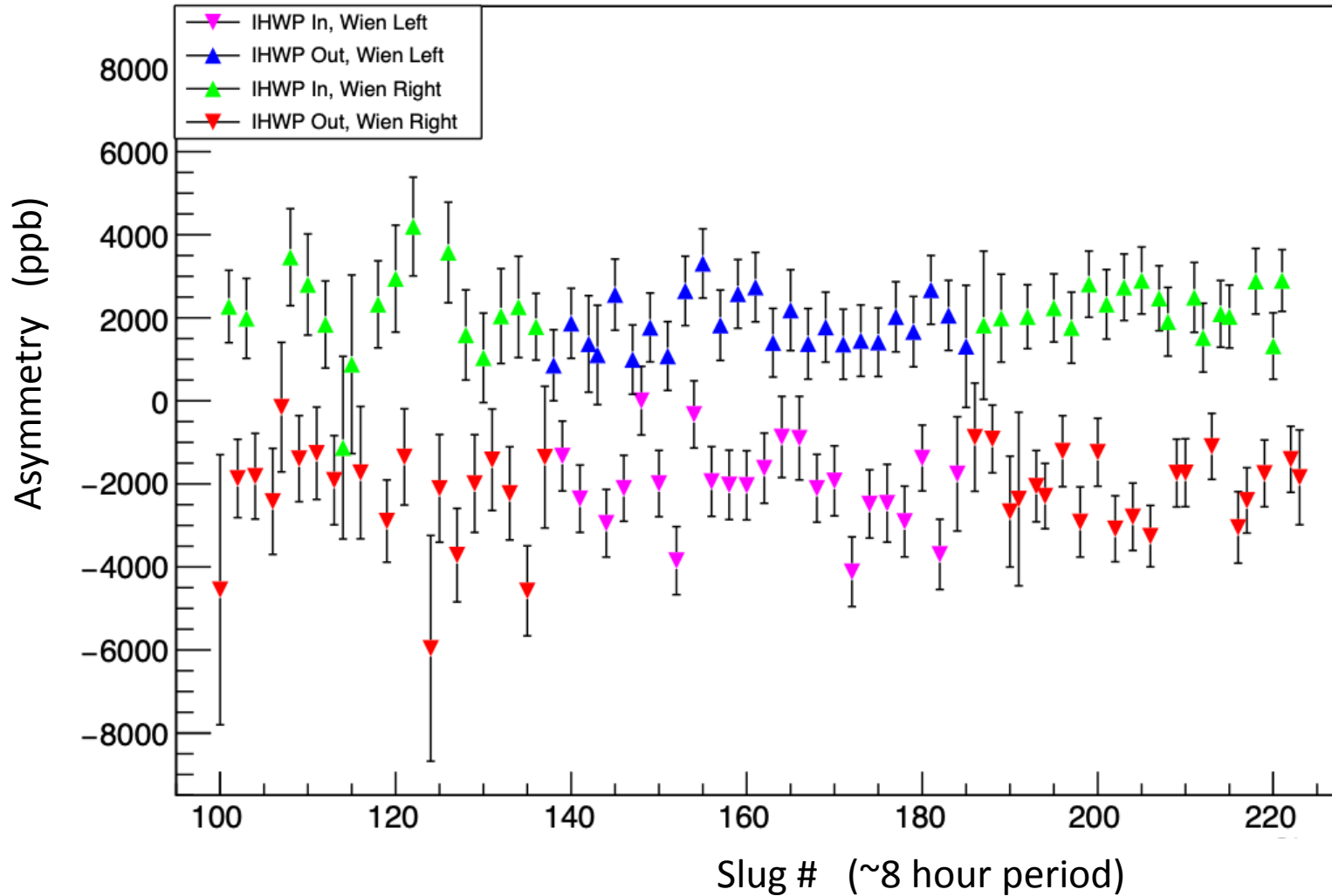
$$A_{phys} = R_{radcorr} R_{accept} R_{Q^2} \frac{A_{corr} - P_L \sum_i f_i A_i}{P_L (1 - \sum_i f_i)}$$

$$A_{corr} = A_{det} - A_{beam} - A_{trans} - A_{nonlin} - A_{blind}$$

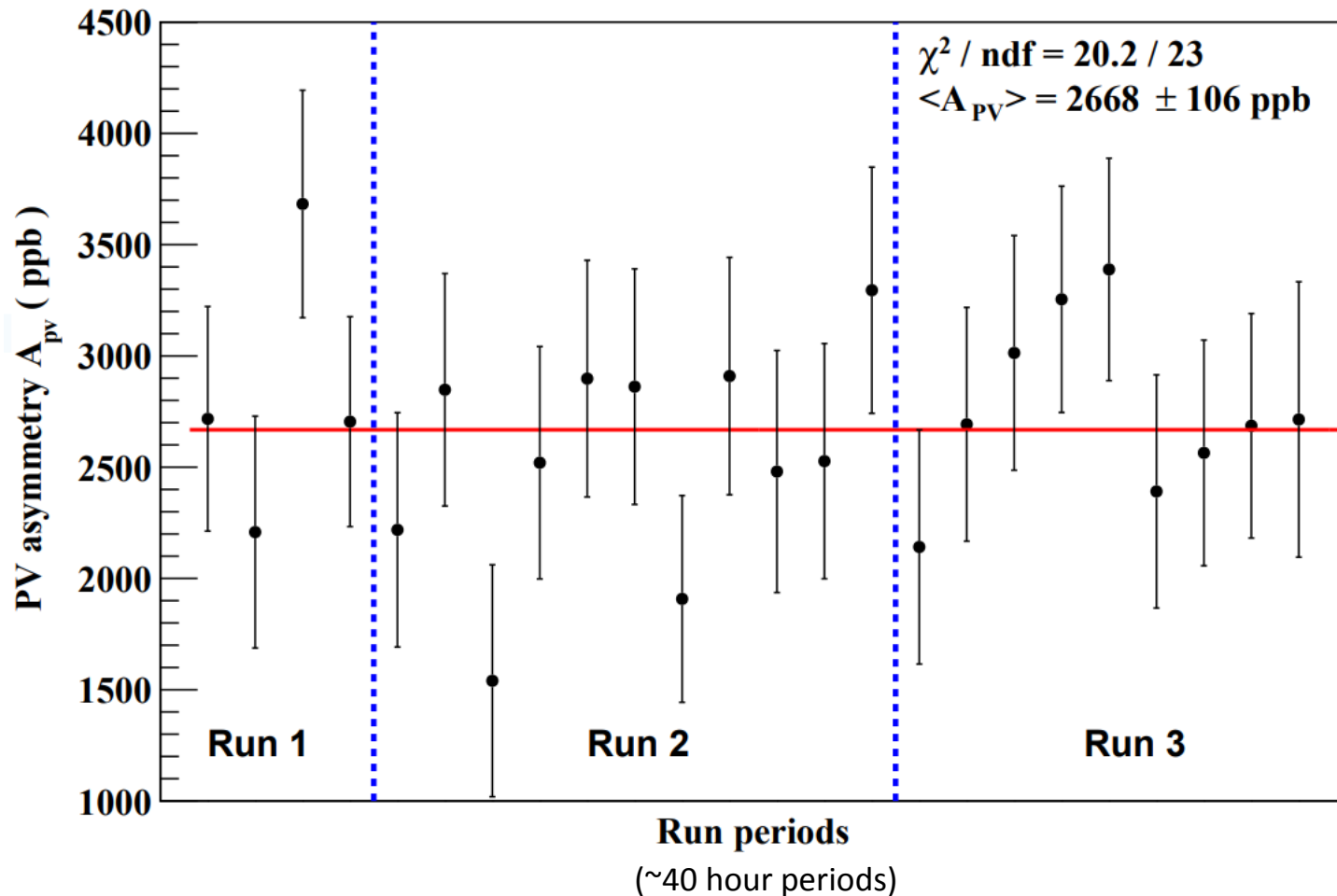
A_{phys} extraction requires effort on multiple fronts:

- $R_{radcorr}$ (radiative correction)
- R_{accept} (acceptance)
- R_{Q^2} (Q^2 -scaling)
- P_L (beam polarization)
- $\frac{1}{1 - \sum_i f_i}$ (Overall background dilution)
- $P_L \sum_i f_i A_i$ (backgrounds)
- A_{corr} (Corrected Asymmetry)
- A_{beam} (Beam corrections)
- A_{trans} (Transverse asymmetry correction)
- A_{nonlin} (Detector nonlinearity)
- A_{blind} (Blinding factor)

^{48}Ca Asymmetry Measurements

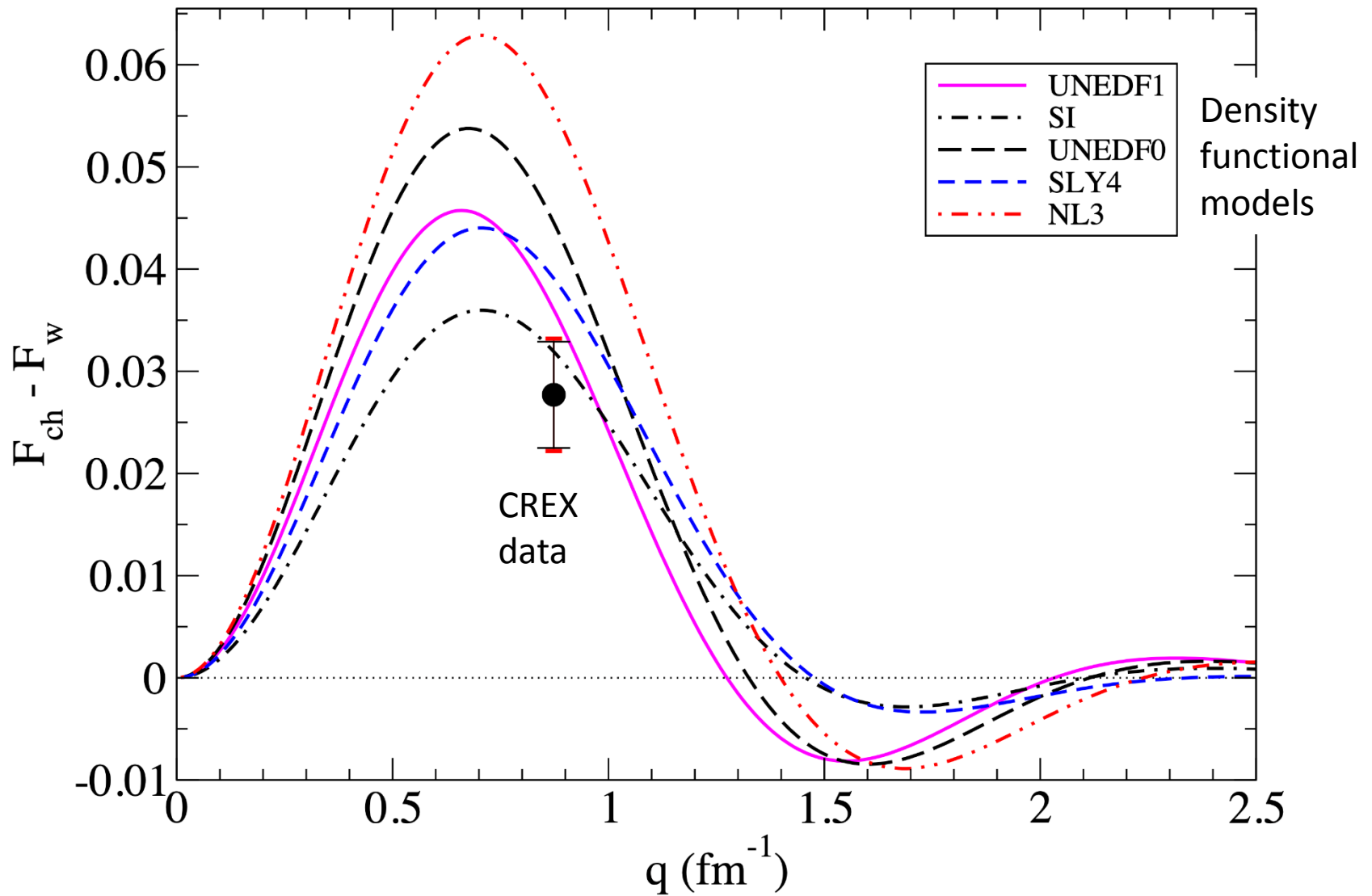


^{48}Ca Asymmetry Measurements



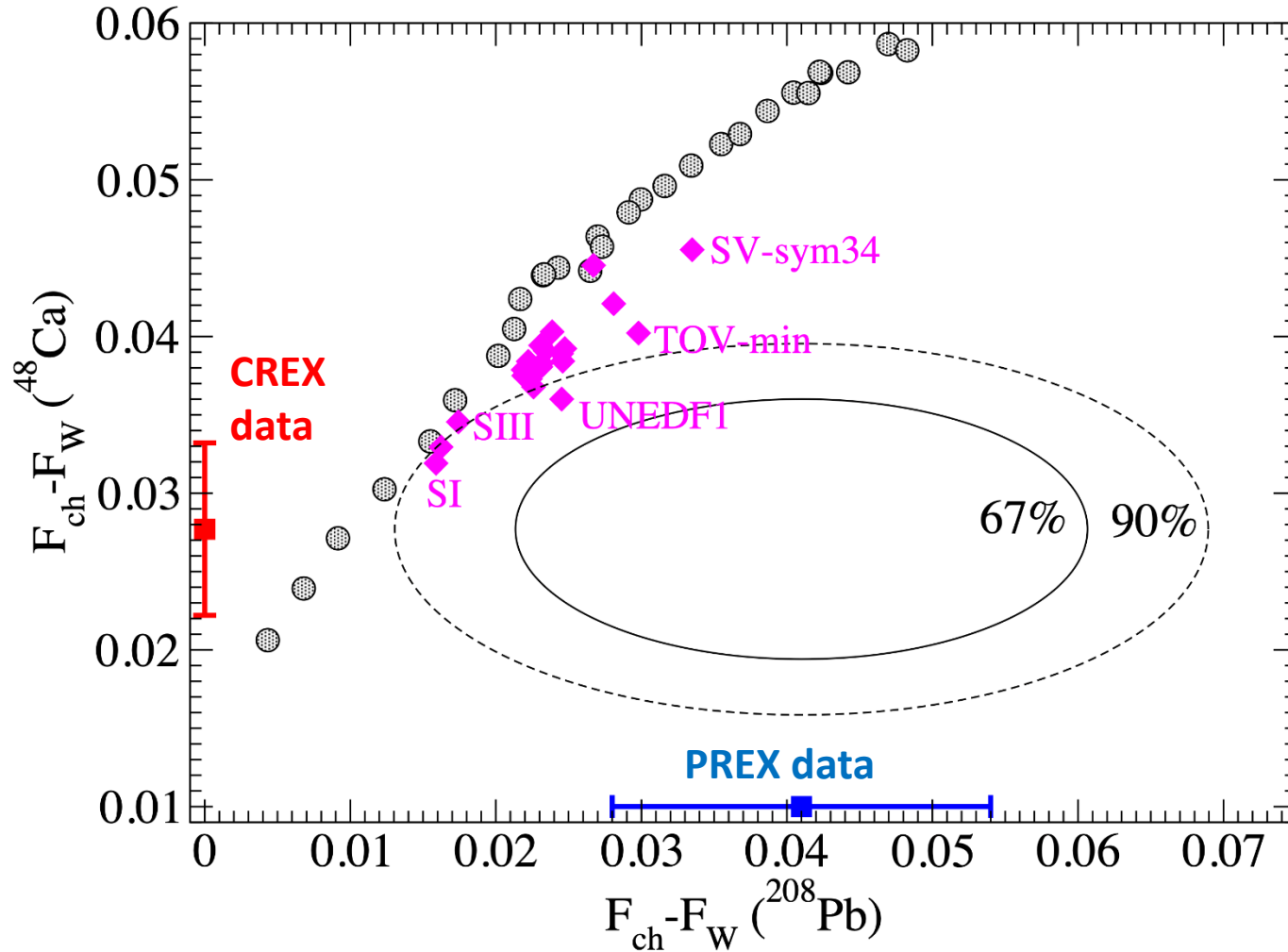
Three run periods demarcate injector spin orientation reversals.

Difference between charge and weak form factor for ^{48}Ca



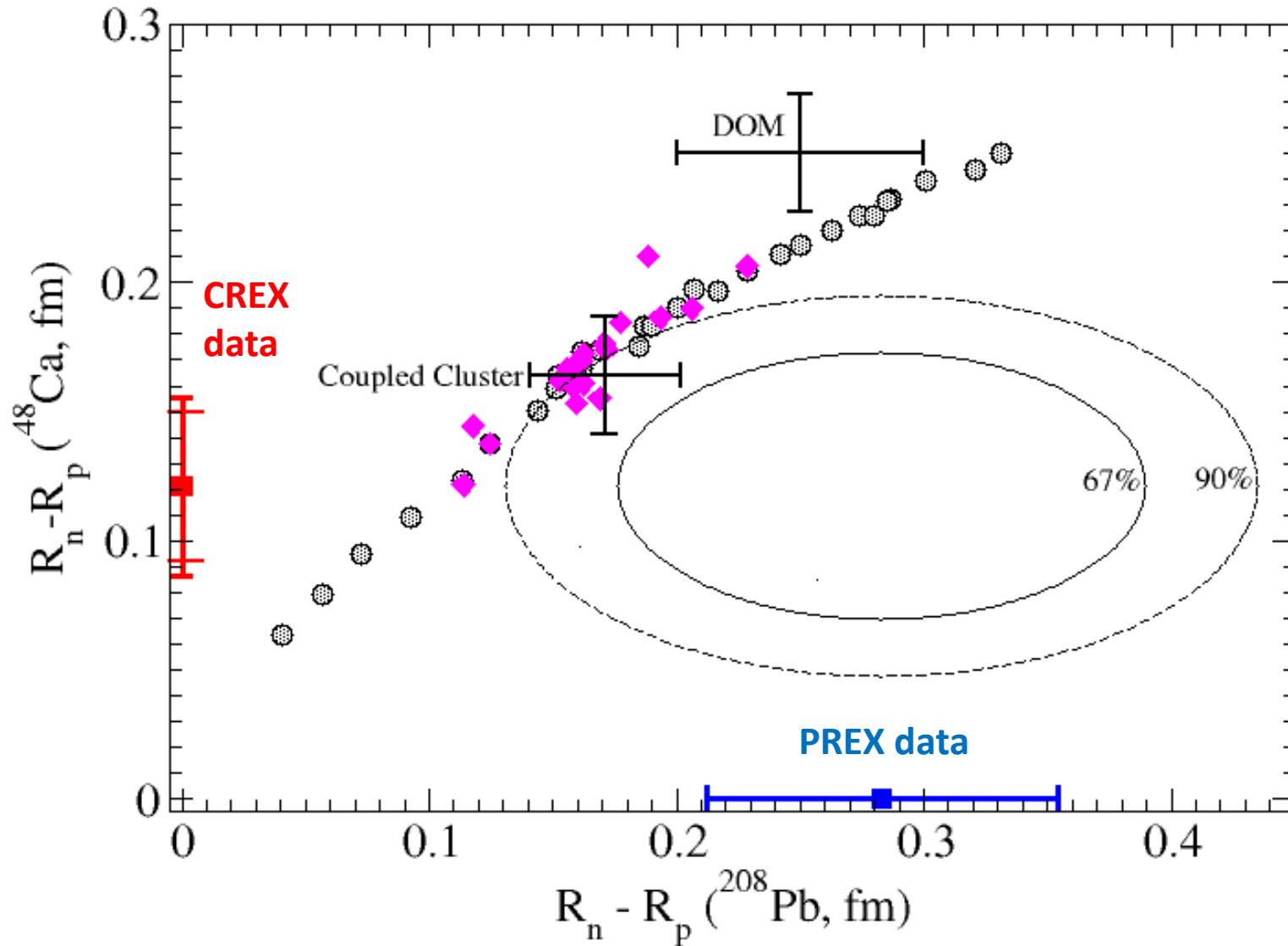
Weak Form Factor -- Model Independent

Comparing PREX (^{208}Pb) and CREX (^{48}Ca) to Theory



Neutron Skins -- Has a small model dependence

Neutron Skins vs Theory



PREX/CREX Related Publications

Recent or Planned

Authored by the PREX collaboration or by subsets of it.

- CREX PRL 129, 042501 (2022)
- PREX-2 PRL 126, 172502 (2021)
- SSA PRL 128 14, (2022)
- Moller polarimeter D.E. King et al, NIM.A 1045 (2023) 167506.
- Compton polarimeter (planned)
- Polarized source and beam P.A. Adderley et al, NIM.A 1046 (2023) 167710.
- Phys Rev C archival paper (draft)
- Target NIM (draft)
- Quartz detector and PMT non-linearity NIM (planned)
- New analysis methods (planned)
- Theory (inelastics, extracting skins)

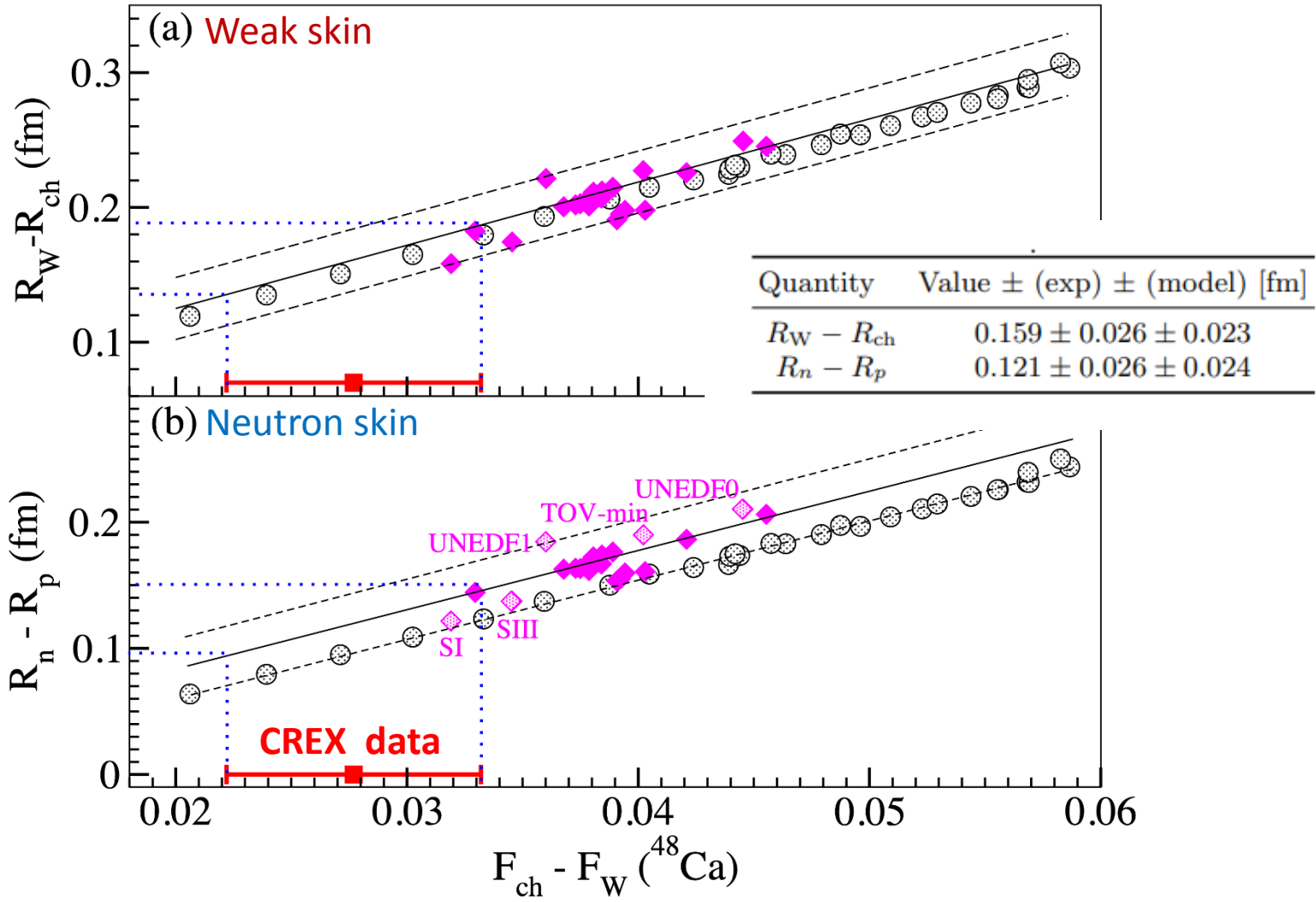
Conclusions

- New and precise measurement of the PVES Asymmetry from ^{48}Ca
 - Model-independent extraction of the **weak form factor** at $q = 0.8733 \text{ fm}^{-1}$
 - Weak Skin and Neutron Skin extracted (w/ small model dependence).
 - ^{48}Ca : **thin skin**
 - ^{208}Pb : **thick skin**
- } compared to models
- Consistent with a number of DFT models and with microscopic coupled-cluster model

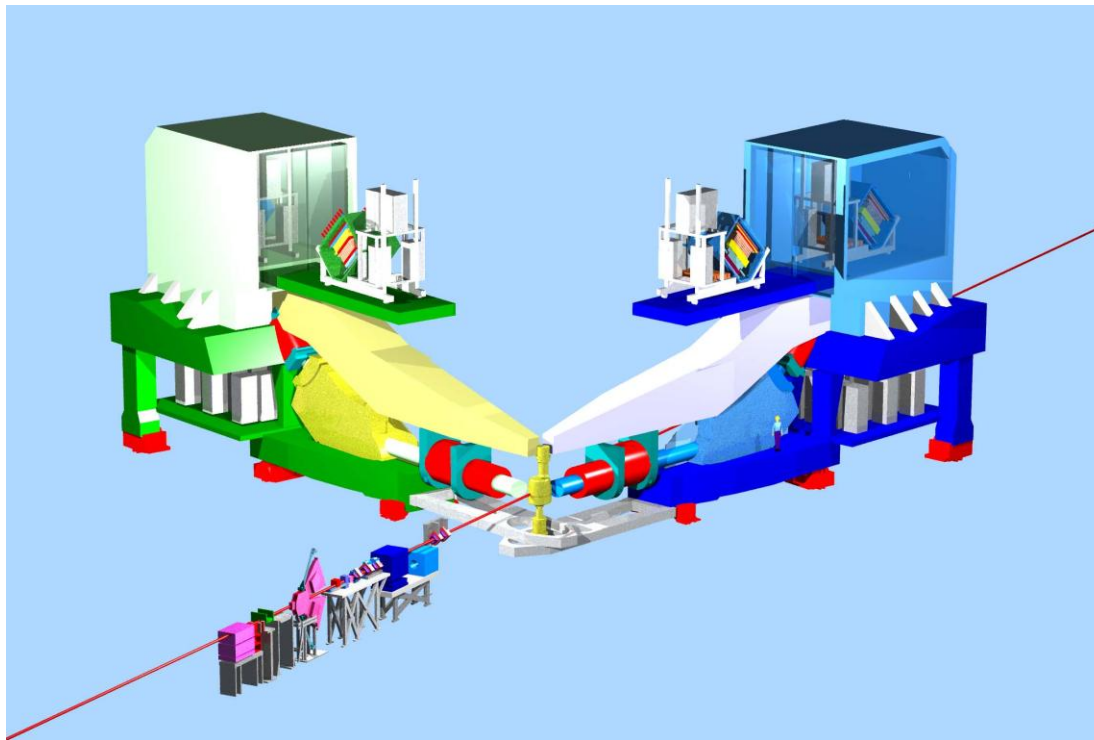
<http://hallaweb.jlab.org/parity/prex>

Backup Material

^{48}Ca Weak minus charge rms radius vs charge minus weak form factor (top), and neutron minus proton radius (bottom)



High Resolution Spectrometers



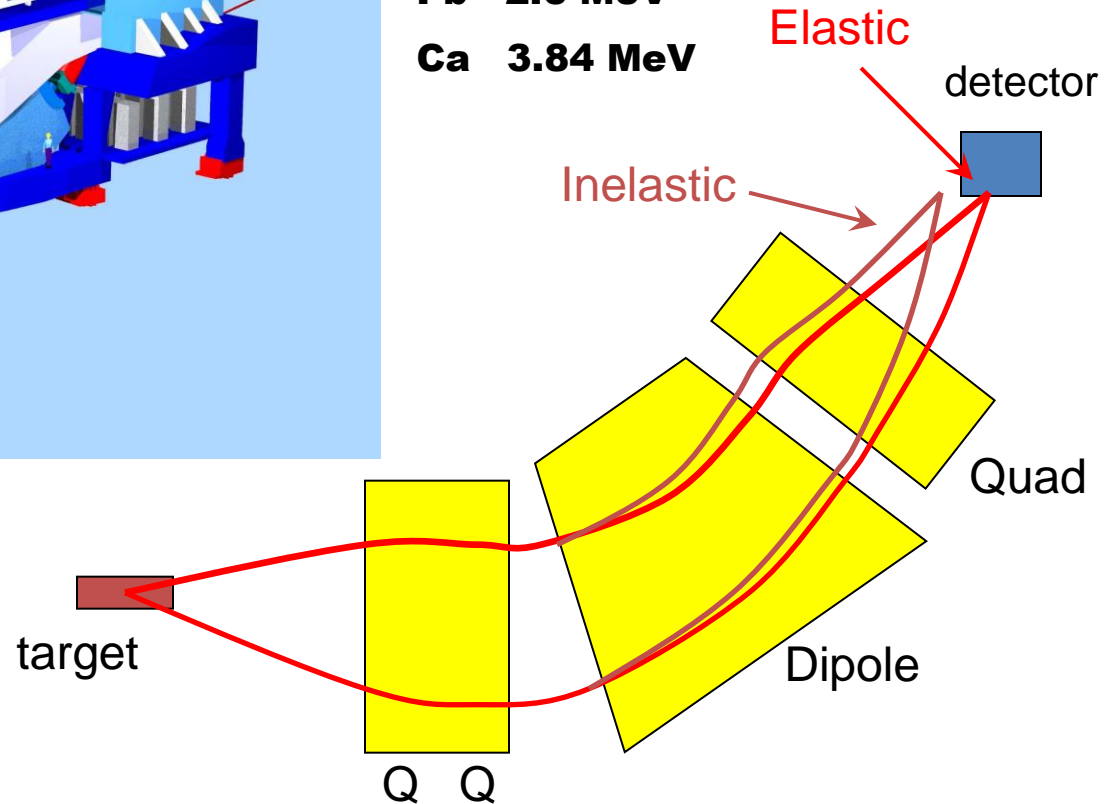
Left-Right symmetry to control transverse polarization systematic

Spectrometer Concept:
Resolve Elastic

1st excited state

Pb 2.6 MeV

Ca 3.84 MeV

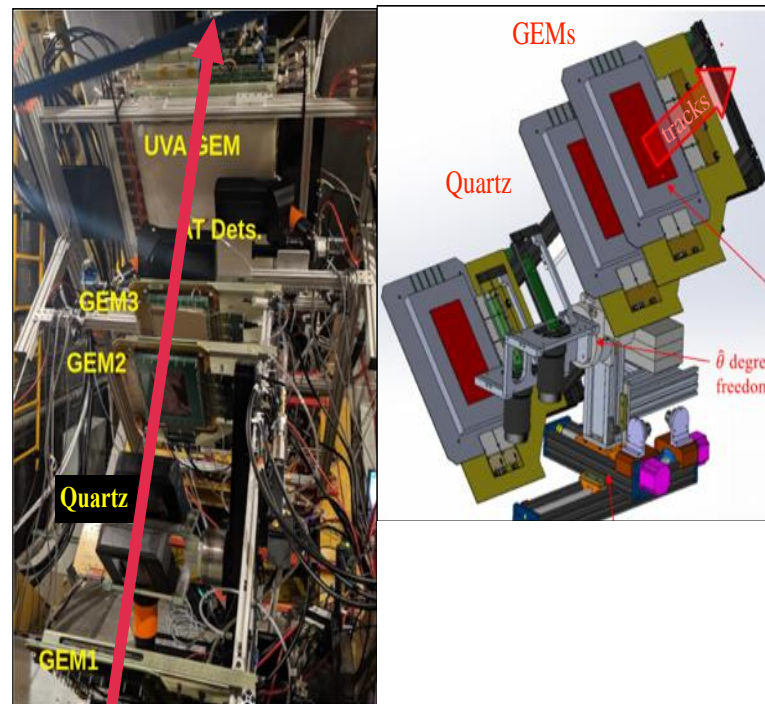


Integrating Detectors



- The challenge: all electrons need to count the same - high photon statistics but low shower fluctuations
- Fused silica Cerenkov radiator, 5mm thick, 3.5x16 cm² area, mated to a single PMT
- ~56 MHz signal rate in a 3x3 cm² area at the end of the detector
- Non-linearity of detector response was tested on the bench and with beam during the experiment

Counting Detectors



- The HRS Vertical Drift Chambers (VDCs) below the quartz detectors
- GEMs that we installed upstream and downstream of our quartz detectors
- Used to align the elastic peak on the quartz and to measure accepted kinematics
- Used at very low beam currents (<1uA) “counting experimental mode”

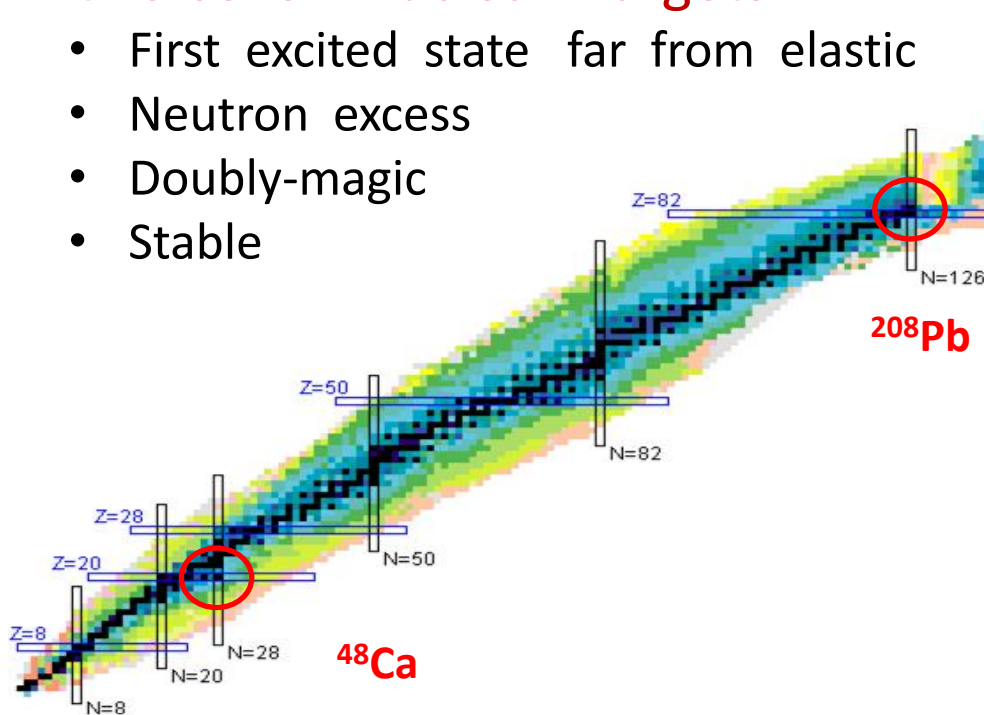
Neutron form factor

$$A \approx \frac{G_F Q^2}{2\pi\alpha\sqrt{2}} \left[1 - 4\sin^2\theta_W - \frac{F_N(Q^2)}{F_P(Q^2)} \right]$$

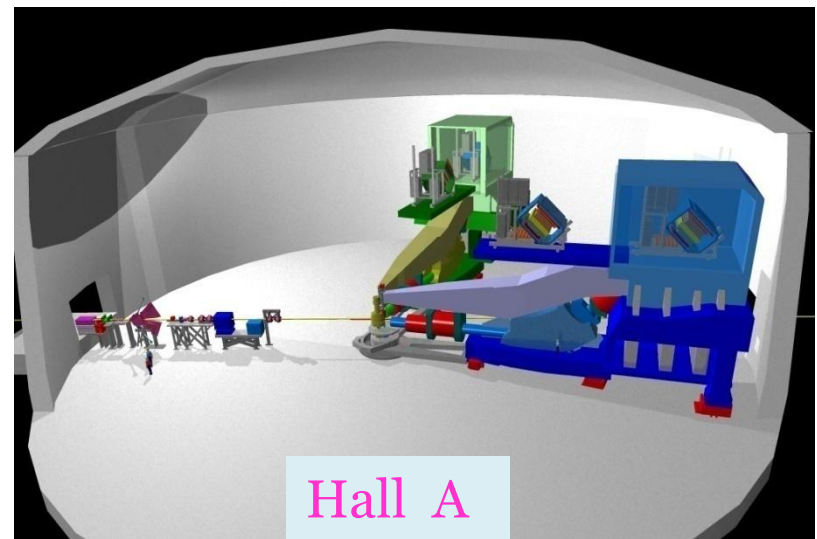


Choice of Nuclear Targets

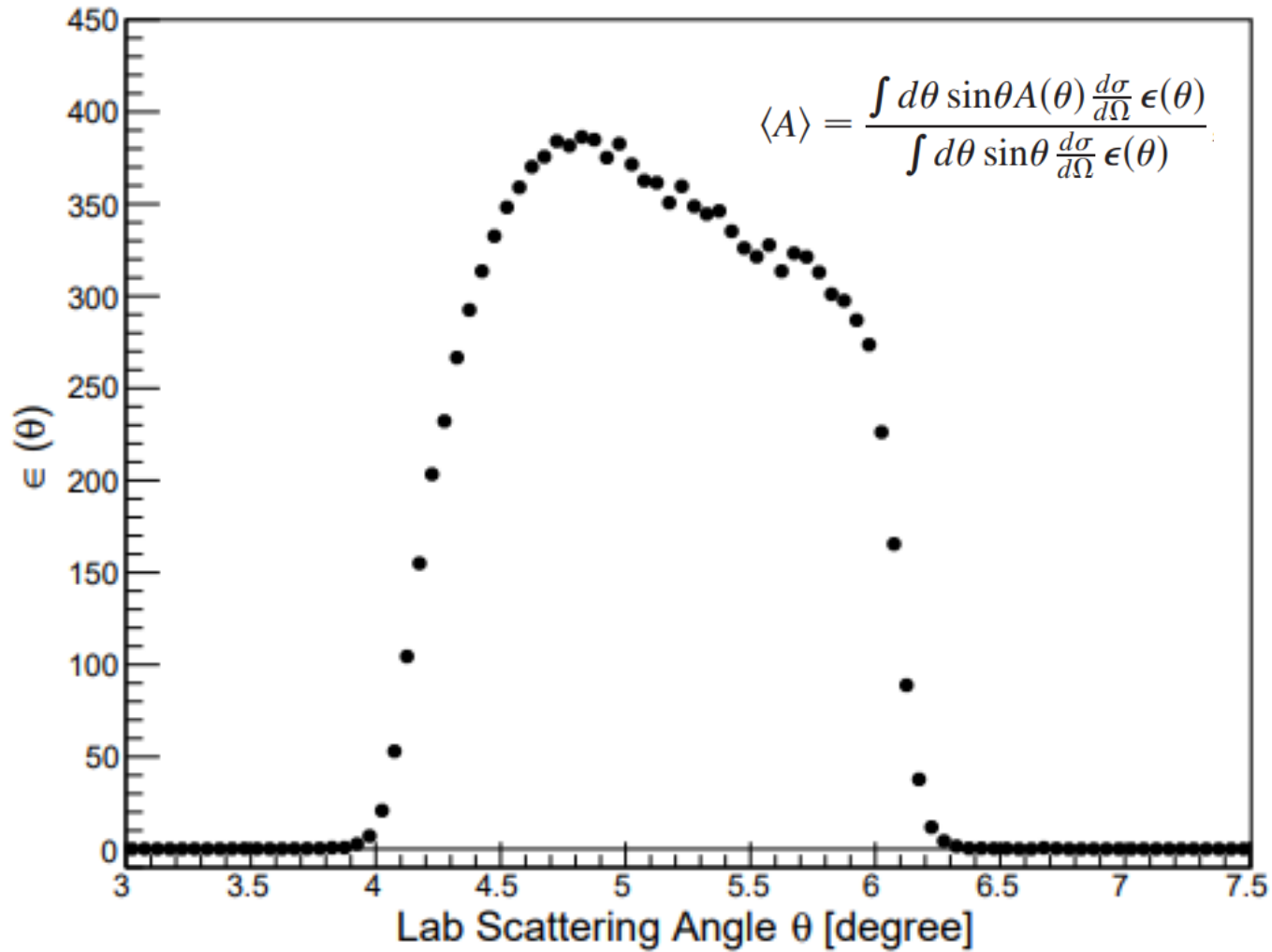
- First excited state far from elastic
- Neutron excess
- Doubly-magic
- Stable



High Resolution (10^{-4}) Spectrometers

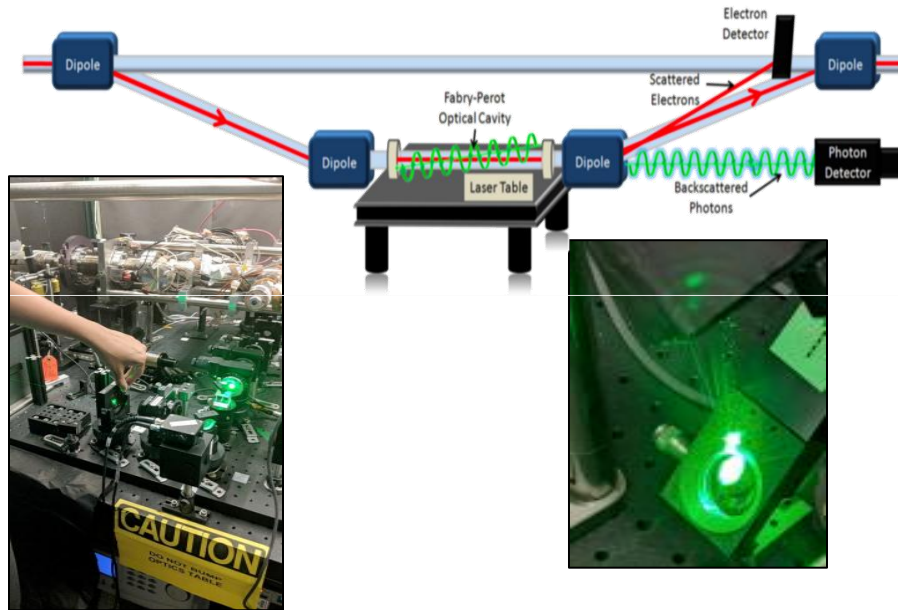


Acceptance Function

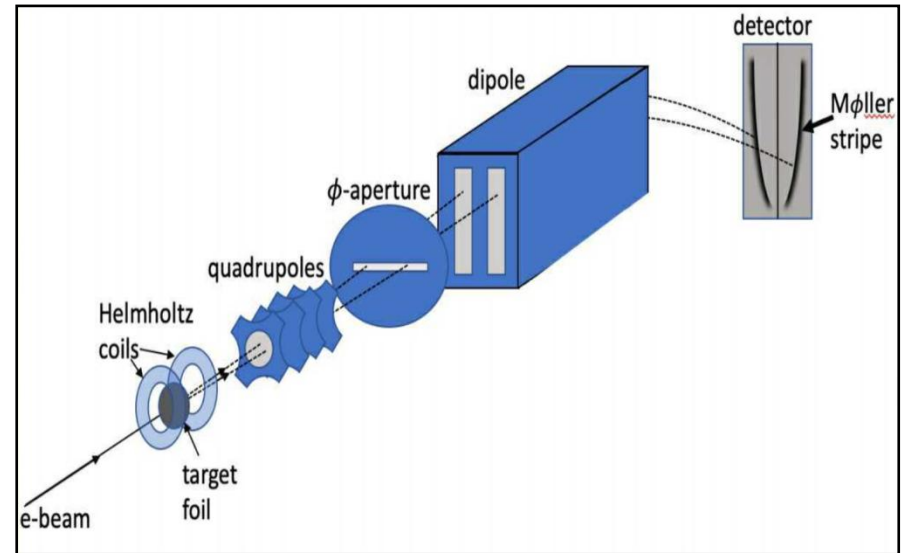


Beam Polarimetry

Compton Polarimetry



Moller Polarimetry



Acknowledgments: S. Malace, E. King, D. Jones, P. Souder

Acknowledgments: A.J. Zec, J. C. Cornejo, M. Dalton, C. Gal, D. Gaskell, C. Palatchi, K. Paschke, A. Premithilake, B. Quinn

- Continuous, non-invasive measurement
- Utilized integrating technique with photon detector
- Evaluated systematic uncertainty
- Polarimeter runs taken continuously alongside main detector data

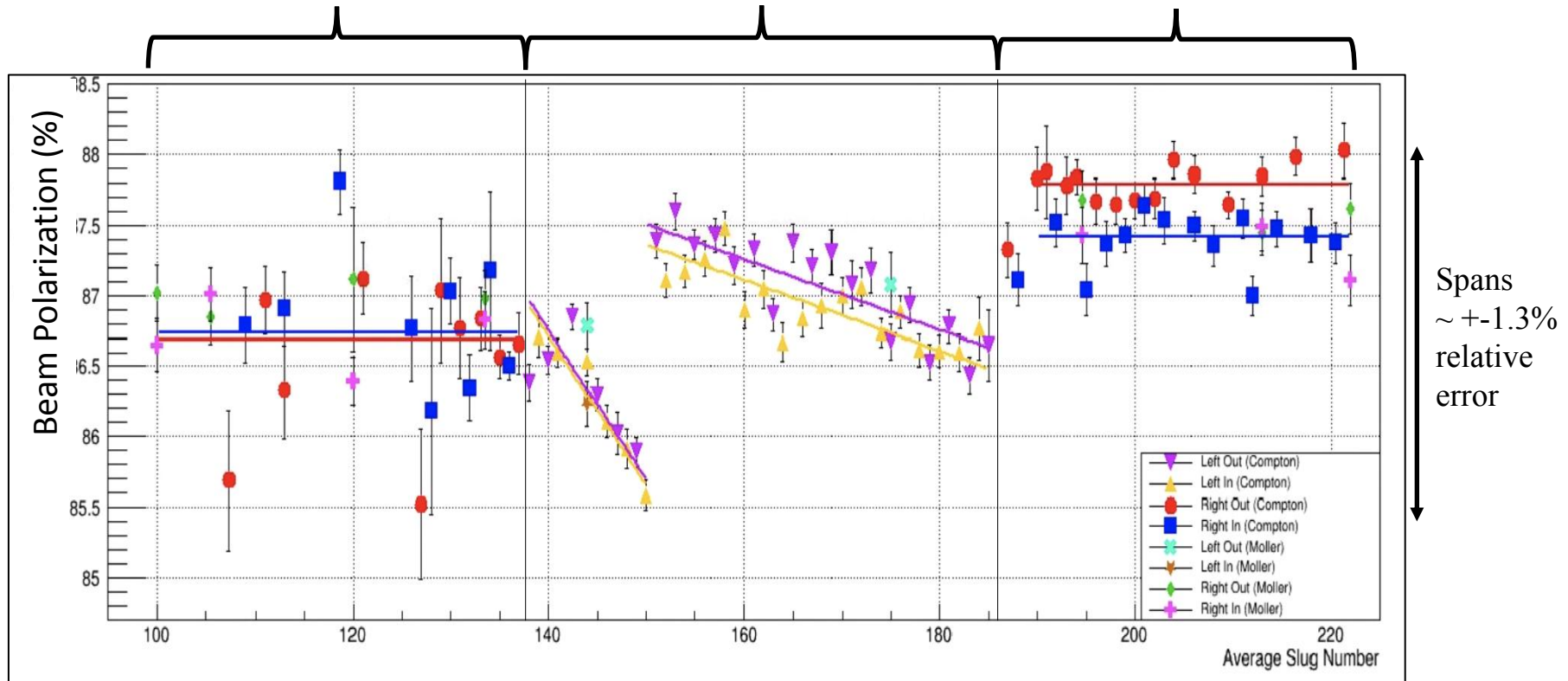
- Low-current, invasive measurement
- 3-4T field provides saturated magnetization perpendicular to the foil
- Spectrometer redesigned for 11 GeV
- CREX reoptimized the spectrometer tune (and detector configuration), to provide high precision and sensitivity to systematic effects
- Polarimeter runs were taken approximately every week

Compton and Moller polarimeter results

1st period Spring 2020
Right (In/Out)

2nd period Spring 2020
Left (In/Out)

3rd period Summer 2020
Right (In/Out)



Acknowledgments: A.J. Zec, J. C. Cornejo, M. Dalton, C. Gal, D. Gaskell, C. Palatchi, K. Paschke, A. Premithilake, B. Quinn

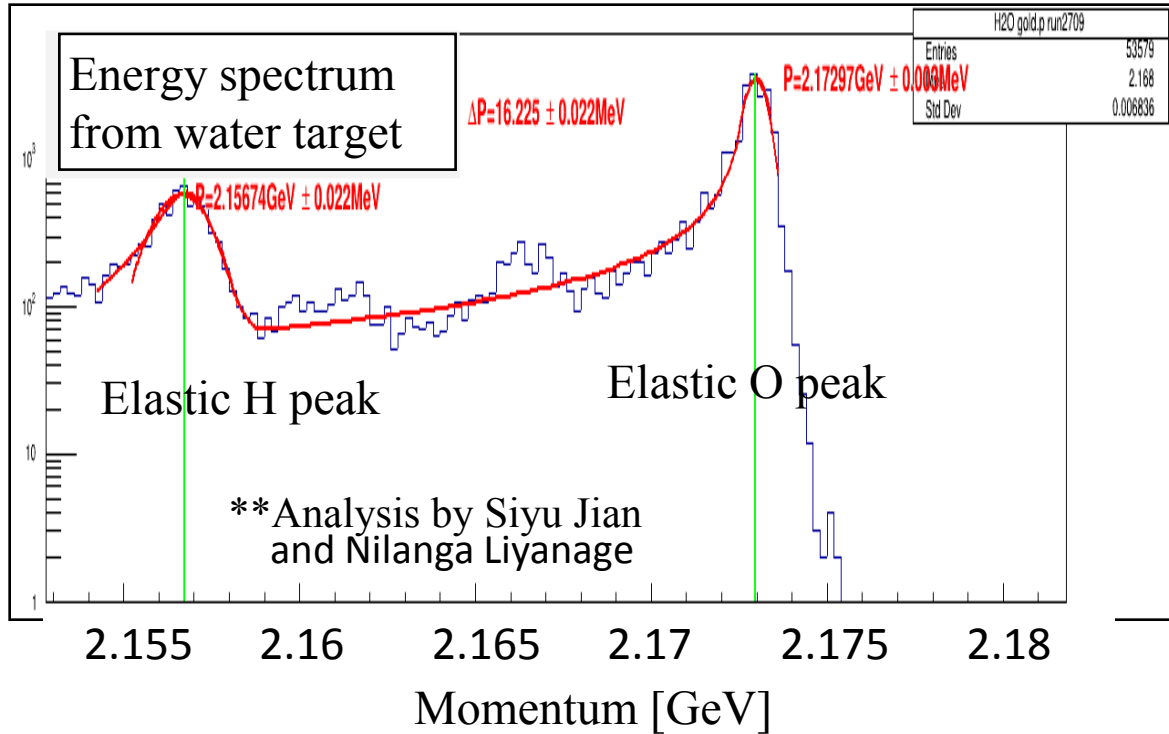
Average Compton polarization:
 $87.10 \pm (0.52\% \text{ dP/P})$

Average Moller polarization:
 $87.06 \pm (0.85\% \text{ dP/P})$

CREX Polarimetry Result:
 $P_e = 87.09 \pm (0.44\% \text{ dP/P})$

This precision is a world record.

Scattering angle calibration with water cell



- Nuclear recoil method
- ^1H and ^{16}O in one target (same E-loss) provides measurement of angle θ

$$A_{PV} \approx \frac{G_F Q^2}{4\pi\alpha\sqrt{2}} \frac{Q_W F_W(Q^2)}{Z F_{ch}(Q^2)}$$

Determined central angle with pointing with precision of $\delta\theta = 0.02^\circ$ (0.45%)

recoil momentum difference \rightarrow scattering angle

$$\Delta E' = E'_O - E'_H = E \left(\frac{1}{1 + \frac{2E \sin^2(\frac{\theta}{2})}{M_O}} - \frac{1}{1 + \frac{2E \sin^2(\frac{\theta}{2})}{M_H}} \right)$$

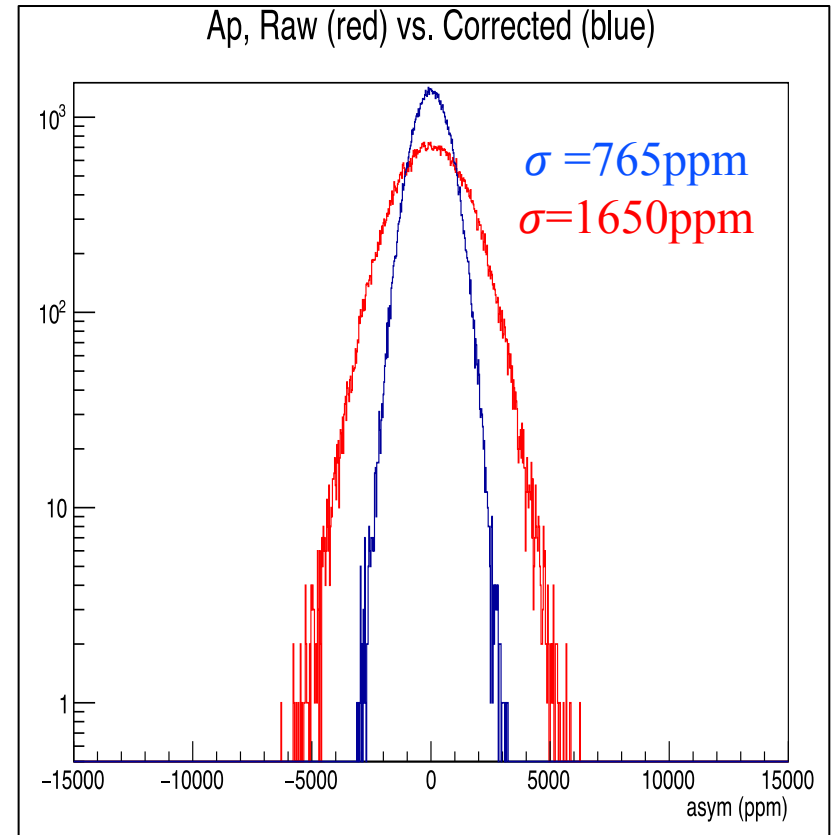
Beam Corrections

Beam jitter noise several times greater than counting statistics

Analysis removes noise and evaluates residual helicity correlations (systematics).

$$A_{\text{raw}} = A_{\text{det}} - A_{\text{Q}} + \alpha \Delta_{\text{E}} + \sum \beta_i \Delta x_i$$

The α for energy is another β for a monitor.



- Potential for systematic error if average beam asymmetries are not well corrected
- Multiple techniques used to calibrate correction factors (β_i)

The Math of Beam Corrections -- 3 Methods

$$A_{\text{raw}} = A_{\text{det}} - A_Q + \alpha \Delta_E + \sum \beta_i \Delta x_i$$

Regression

$$\chi^2 = \sum \left(A_{\text{raw}} - \sum_i \beta_i \Delta M_i \right)^2, \quad \frac{\partial \chi^2}{\partial \beta_i} = 0$$

The α for energy is another β for a monitor.

Dithering

$$\frac{\partial \bar{D}}{\partial C_\mu} = \sum_{i=1}^{N_{BPM}} \beta_i \frac{\partial M_i}{\partial C_\mu}, \quad \beta_i = \frac{\partial \hat{D}}{\partial M_i},$$

for $\mu = 1, 2, \dots, N_{\text{coil}}$, **and can be solved if**

$$N_{\text{coil}} \geq N_{BPM}.$$

Lagrange -- a combination of the above two

$$\mathcal{L} = \chi^2 + \sum_{\mu} \lambda_{\mu} \left(\frac{\partial D}{\partial C_{\mu}} - \sum_i \beta_i \frac{\partial M_i}{\partial C_{\mu}} \right),$$

χ^2 **minimization** with **beam modulation sensitivities constraints:**

$$\frac{\partial \mathcal{L}}{\partial \beta_i} = 0, \quad \frac{\partial \mathcal{L}}{\partial \lambda_{\mu}} = 0$$

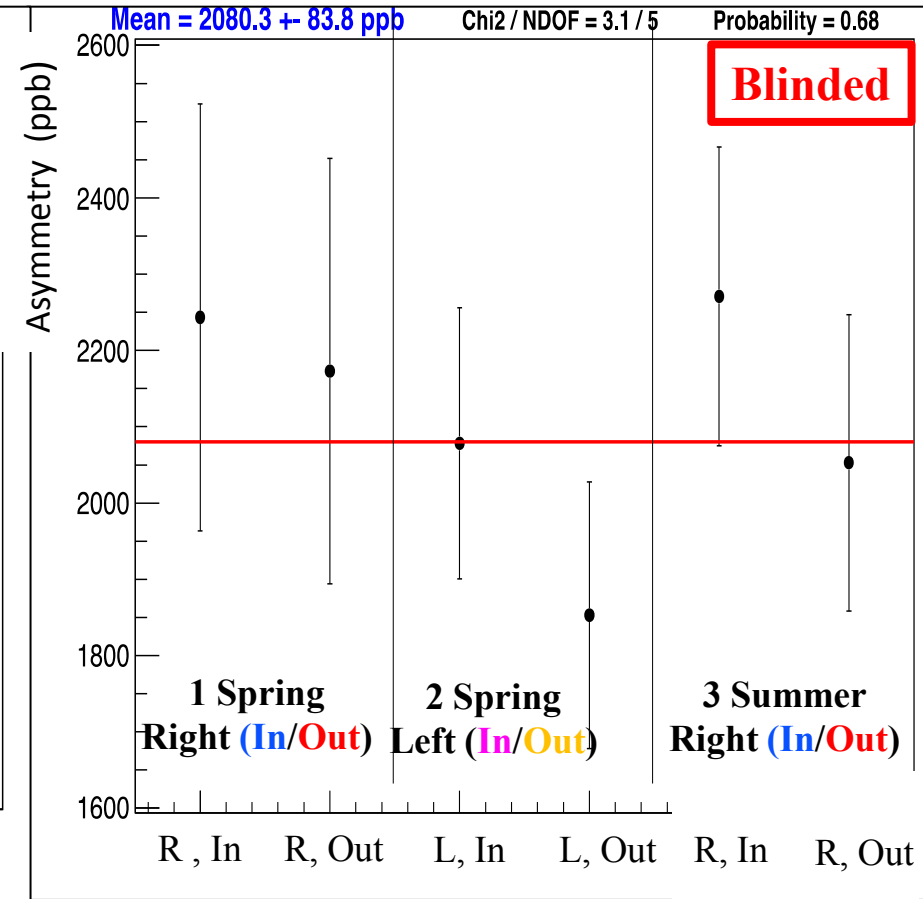
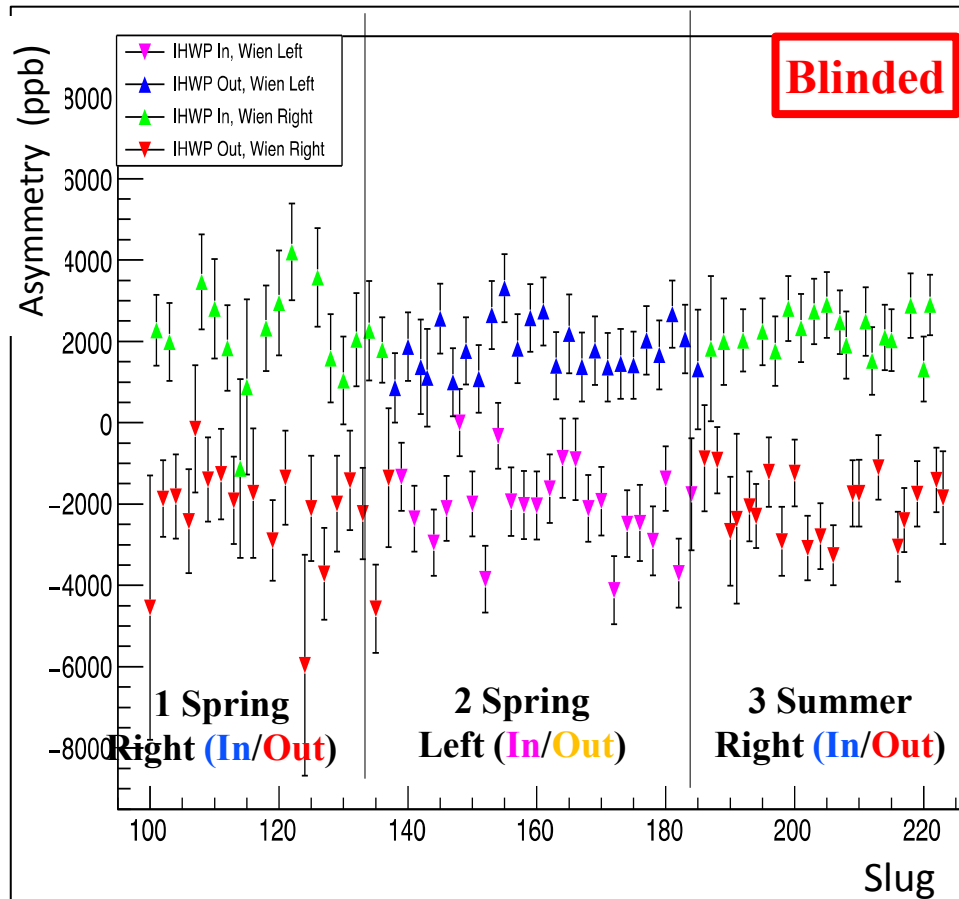
Credit: Paul Souder,
Tao Ye, Kent Paschke,
Cameron Clarke, Ye
Tian, Victoria Owen

Beam corrected (but still blinded) Asymmetries

Half Wave Plate: IN/OUT Wien(Spin Manipulator): Left/Right

Sign-uncorrected, Each point: 8h time-scale

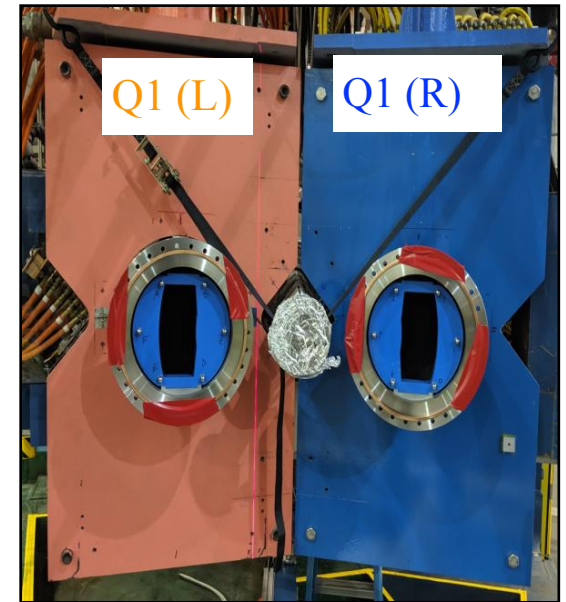
Sign-corrected, Each point: ~1 week time-scale



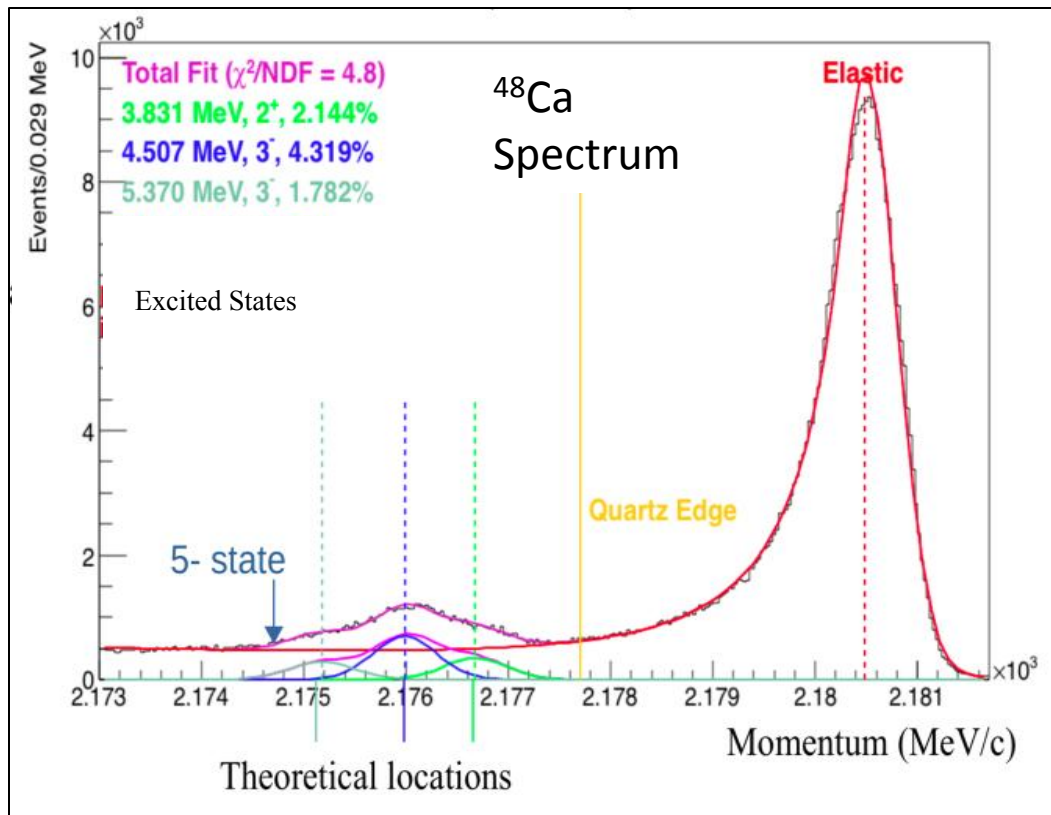
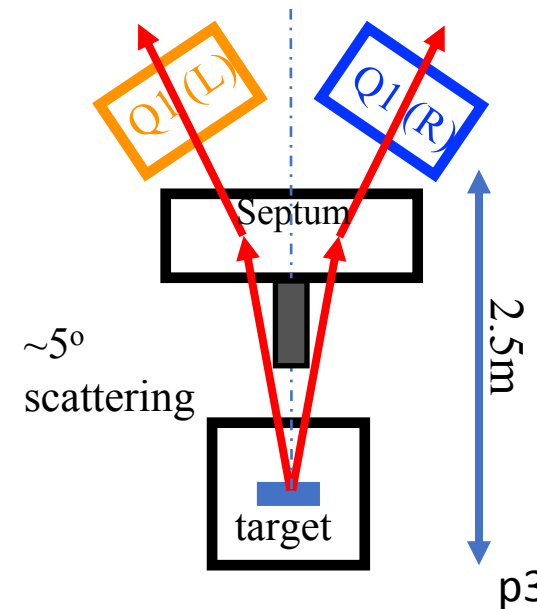
- Entire data set! 6 colors on left correspond to 6 points on the right (zoomed in y-scale)
- Measuring continuously flipping sign by 2 methods (IHWP, Wien)
- The corrected asymmetry removed effects from beam asymmetries and noise

High Resolution Spectrometers -- HRS

- Spectrometer separates elastic peak, directs it onto integrating detector (quartz).
- Integrate detector in each of the spectrometer pair independently



~12.5° Spectrometers



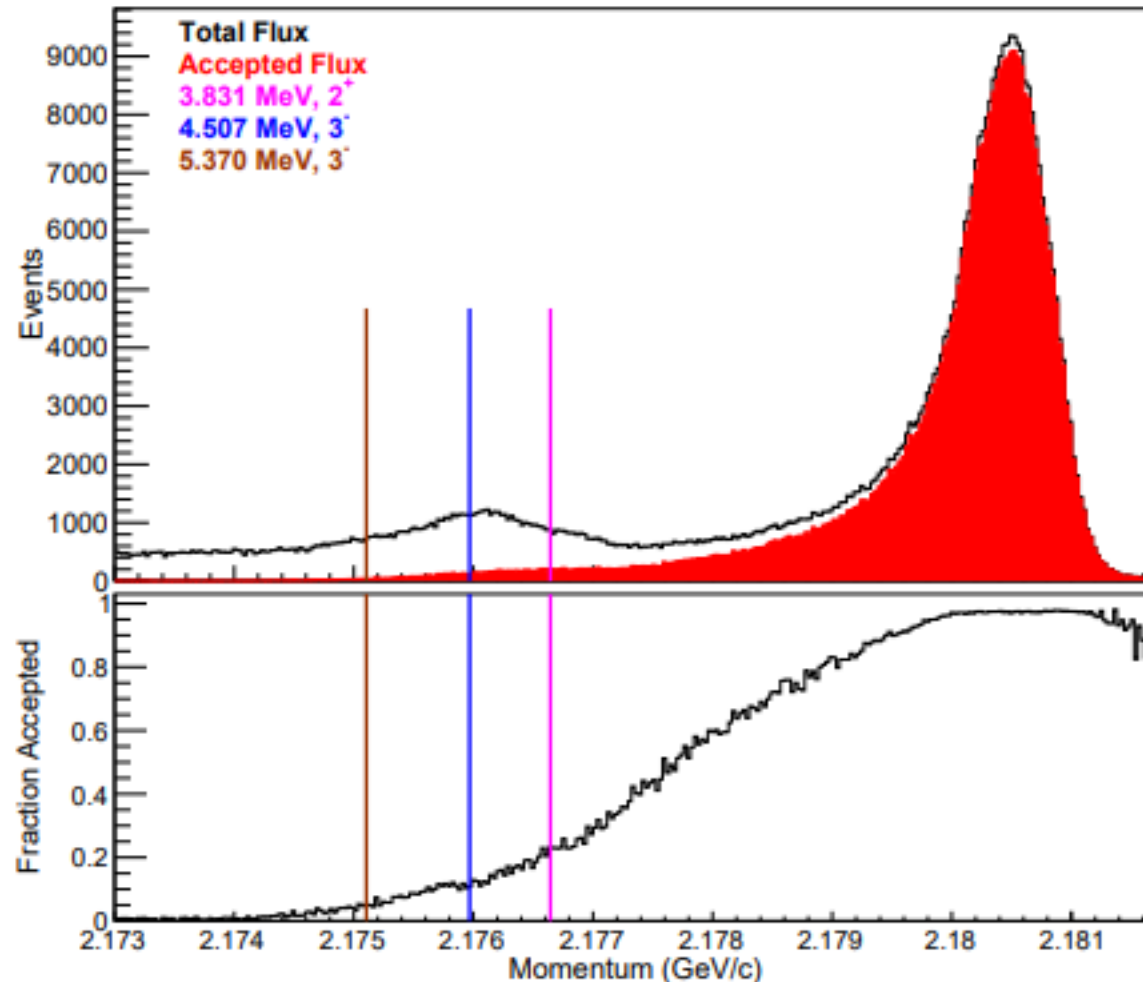


FIG. 3. Momentum spectrum in the spectrometer (top) and acceptance as a function of momentum in the spectrometer (bottom). The significant inelastic levels are marked. Shaded region in the momentum spectrum registered pulses in the integrating detector.